

For use in photovoltaic applications, high voltage gain hybrid boost converter mathematical modelling

Muhammad Salman Khan^{*}, Ahmad Wali¹, Muhammad Ismail², Atta Ur Rehman², Muhammad Afzaal²
Muhammad Sabeel Shah³

^{*}Department of Electrical Engineering University of Engineering and Technology Peshawar, Pakistan.

¹Sarhad University of Science and Information Technology Peshawar, Pakistan

²Department of Electrical Engineering University of Engineering and Technology Mardan, Pakistan

³Electrical Automation Department National Institute of Electronics Islamabad, Pakistan

**(13bnele0598@uetpeshawar.edu.pk)*

(Received: 13 October 2023, Accepted: 23 October 2023)

(2nd International Conference on Recent Academic Studies ICRAS 2023, October 19-20, 2023)

ATIF/REFERENCE: Khan, M. S., Wali, A., Ismail, M., Rehman, A. U., Afzaal, M. & Shah, M. S. (2023). For use in photovoltaic applications, high voltage gain hybrid boost converter mathematical modelling. *International Journal of Advanced Natural Sciences and Engineering Researches*, 7(10), 97-103.

Abstract –On this research, a high voltage-gain Hybrid boost converter (HVBHC) is developed to achieve high voltage gain, good transient responsiveness, low voltage ripples, and sufficient efficiency when compared to a basic conventional boost converter and to lower the harmonic content on the output side. The suggested topology's voltage gain is 96% at a duty ratio of 0.55 and a frequency of 50 KHz. The suggested converter's circuit schematic has a switched inductor and switch capacitor architecture. As a result, the inductor reduces the voltage stress on the active switch, the output voltage of the proposed converter is high, and the reaction of different parameters is examined using the simulation tool PSIM.

Keywords – Include, Boost Converter, Duty Cycle, Continues Conduction Mode (CCM), Switched Inductor, Switched Capacitor

I. INTRODUCTION

Globally, the energy situation has recently gotten worse by the day. Among all renewable energy sources, solar PV (Photovoltaic) technology is one of the most dependable methods for producing power. Numerous benefits of this technology include its lack of noise, reduced environmental impact, lack of moving components, and ease of use. This study first proposes mathematical modelling of a high voltage gain hybrid boost converter, which is guaranteed to raise voltage from 12V to 47V [1]. The cost of installing a solar power system is quite expensive. Therefore, the price of PV installation may be decreased by improving manufacturing technologies and solar power generating efficiency. Utilizing our finite energy resources to run electrical equipment effectively is a crucial aspect of electrical

and electronics engineering [2]. Such a current may lead to increased weight, cost, and power losses. To increase efficiency and lower overall leakage current, the converter without a transformer is being studied. We provide a high static gain hybrid DC/DC converter with a single switch that is appropriate for solar applications. To maximize voltage-gain and lower voltage across all power components, the suggested design includes two standard DC/DC converters [3,4]. As a consequence, this converter may be used in a two-stage DC module layout without a mid-point transformer to link to a voltage source inverter [5]. To offer a large step-up voltage gain while keeping a low duty ratio, many topologies have been suggested [6,7]. But each of these varieties is more-costly and difficult. good voltage-gain, low voltage stress on the active switch, and

excellent transient responsiveness, minimal voltage ripples, adequate efficiency, high voltage gain, and low voltage stress across the switch as compared to a straightforward traditional boost converter. The circuit schematic for the High Voltage Gain Hybrid Boost Converter (HVVHC) architecture is shown in Fig. 1. A duty cycle D on the PWM signal controls the power transistor's switching.

A power switch that periodically switches to allow electricity to flow from input to output is the foundation of the total conversion. With the exception of one piece of the switched inductor since it only has one electronic switch, the proposed new HVVHC architecture operates similarly to how the converter does. The switch inductor and capacitor cells that replace the capacitor and inductor at the end are the primary distinction between the cuk converter and the recently suggested architecture.

The proposed HVVHC topology has two operational states: ON when switch $S1$ is conducting, and OFF when switch $S1$ is not.

Mode I. The voltage source charges the input inductor in series through Switch S while the switch is conducting. The switch allows the current to return to the source. Inductors receive a simultaneous discharge of the capacitors' stored energy. Since both inductors are the same, the same amount of current passes through both $L1$ and $L2$ inductors. Both inductors have the same amount of energy stored in them. In Fig.2, the entire function is shown.

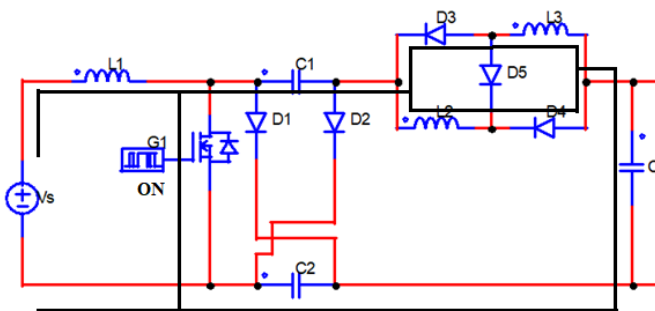


Fig. 2. Mode I

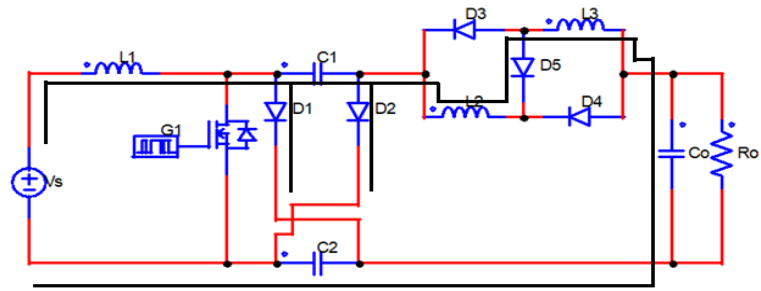


Fig. 3. Mode II

Mode II. The input supply and input inductor $L1$ also charge the capacitors $C1$ & $C2$ and supplies the load, while input supply and input inductor $L1$ also charge the capacitors $C1$ & $C2$ and turn off the diodes $D1$, $D2$, & $D5$ when the switch S is not conducting (turned off). Following the change in polarity on $C1$ and $C2$, the diode $D5$ becomes reverse biased, and the whole energy stored in the capacitors is discharged to C_o , where the output is obtained as illustrated in Fig. 3. When the total of the voltages on the input source, two capacitors, two inductors, and two capacitors equals the voltage on the capacitor C_o . The entire process is recycled, and

the diode D5 is forward biased.

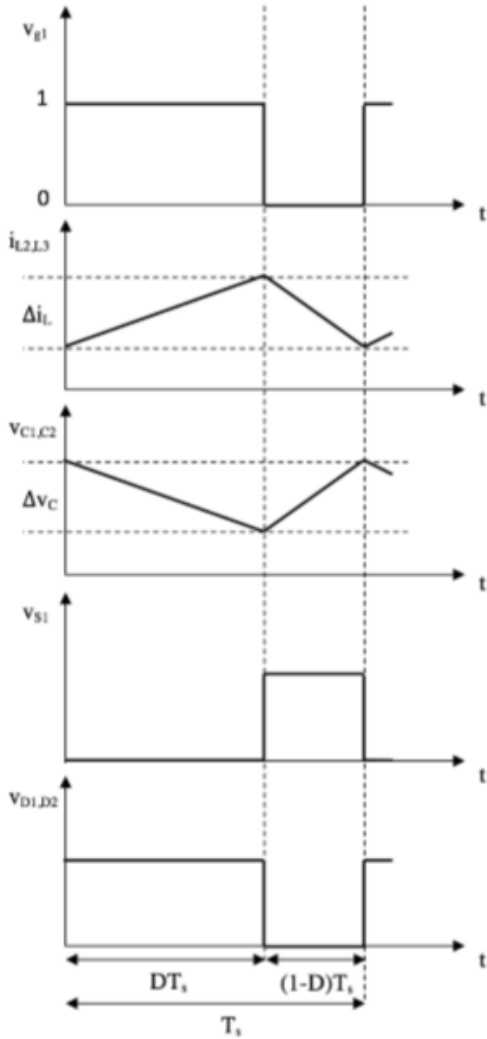


Fig.4. Steady-state waveforms of HVHC topology

In Fig.4, switching diagrams for the SLSC topology's primary steady-state waveforms with increased variations are displayed in CCM.

IV. ANALYSIS OF PROPOSED HVHBC TOPOLOGY

To make the analysis simpler, the suggested converter runs in steady-state. Additionally, it is assumed that every component is perfect (100 percent efficient), that input voltage V_s is pure dc, and that every capacitor is designed to have a negligibly tiny voltage ripple at switching frequency (f_s).

The voltage across inductors L1, L2, and L3 is given as follows when MOSFET S is conducting as seen in Fig. 4.1:

$$V_{L1}(t) = V_s \quad (1)$$

$$V_{L2}(t) = V_{L3}(t) = 2V_C - V_o = V_L \quad (2)$$

$$V_S = V_{L1}(t) = (L1) \cdot \frac{dI_L}{dt} \quad (3)$$

Where $\frac{dI_{L1}}{dt} = \frac{dI_L}{dt}$

The current is therefore written as follows for the circuit's first portion (1):

$$\Delta I_{C(1)} = D \cdot \frac{V_S}{L1} \quad (4)$$

The current in the closed state is now stated as for the second component (2) of the circuit:

$$\Delta I_{C(2)} = D \cdot \frac{2V_C - V_o}{L} \quad (5)$$

Apply the Kirchoff voltage law (KVL) to Figs.1 and 2's circuit to determine the inductor voltage.

$$V_S = V_{L1}(t) + V_C \quad (6)$$

Where V_{C1} is the voltage across capacitor C1 and $V_{L1}(t)$ is the voltage across L1.

$$V_{L1}(t) = V_S - V_C \quad (7)$$

When the switch is not conducting, the inductor voltage second balance for L1 is given by:

$$V_C = \frac{1}{1-D} V_S \quad (8)$$

Where $V_C = V_{C1} = V_{C2}$

$$V_o = \frac{(1+3D)}{(1+D)} V_C \quad (9)$$

By putting Equation, we get:

$$V_o = \frac{(1+3D)}{(1+D)(1-D)} V_S \quad (10)$$

$$\frac{V_o}{V_S} = \frac{(1+3D)}{(1+D)(1-D)} \quad (11)$$

Equation 11 is the required DC voltage gain of the proposed topology

The peak-to-peak variation of the inductor's current at the input ($\nabla I_{L1} = \nabla I_{Lin}$) and output ∇I_{Lo} sides are expressed in (12) and (13), respectively.

$$\nabla I_{Lin} = \frac{DTV_S}{L_{in}} = \frac{DV_S}{fL_{in}} \quad (12)$$

As $\nabla I_{L3} = \nabla I_{L2} = \nabla I_{Lo}$

And

$$\nabla I_{Lo} = \frac{DT(2V_C - V_o)}{L_o} = \frac{D(2V_C - V_o)}{fL_o} \quad (13)$$

The peak-to-peak variation of the capacitor's voltage ($\nabla V_{C1} = \nabla V_{C2} = \nabla V_C$) is expressed in (14) and (15).

$$\nabla V_C = \frac{DTI_{out}}{C} = \frac{DI_{out}}{fC} \quad (14)$$

We can write it also:

$$\nabla V_C = \frac{DP_{out}}{M_{CCM}V_S f C} \quad (15)$$

Where $M_{CCM} = \frac{V_O}{V_S}$

Equation (10) describe the dc gain conversion ratio of the conventional boost converter and HVHBC respectively.

V. CIRCUIT PERFORMNACE ANALYSIS

Table.1. Parameter with its values

Parameters	Values
Input Voltage	12 V
Inductors L1=L2	600 UH
Capacitors C1=C2	22 UF
Output Capacitor Co	22 UF
Output Resistor Ro	10 Ohm
Duty Cycle D	55%
Voltage Stress Vsw	49 V
Output Power Pout	194 watt
Switching Frequency	50 KHz
Input Power Pin	202 watt
output voltage Vo	47 V

Several simulation experiments were carried out to verify the correctness of the theoretical analysis of the proposed High Voltage Gain Hybrid Boost Converter (HVHBC) topology in Continuous Conduction Mode (CCM) and Discontinuous Conduction Mode (DCM) and to assess the performance of the entire circuit. The simulations were run using PSIM, a programme that is often used in the field of power engineering. On the basis of the parameters listed in Table 1, the High Voltage Gain Hybrid Boost Converter (HVHBC) architecture was modelled.

With a duty cycle of 55% and an output voltage of 47 volts, the input voltage is 12 volts. At 50 kHz, which is the switching frequency, these parameters were selected.

A. INPUT CURRENT AND VOLTAGE

Using the PSIM programme, Fig. 4.1(a) displays the input voltage and current. When the switch is in the ON position, the input inductor is charged in series. As a result, the input current is 16.88 A, and

when a switch is turned off, the input current drops to 50% of its original amount.

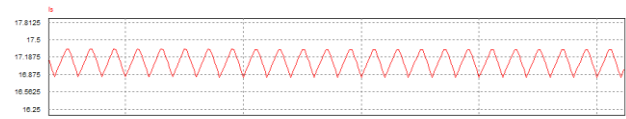


Fig.4.1 (a) Input Current

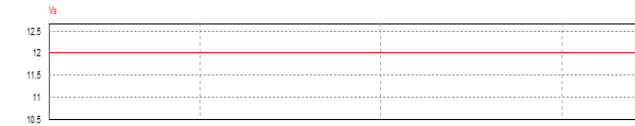


Fig. 4.1 (b) Input Voltage

B. OUTPUT CURENT AND VOLTAGE

In Fig.4.2(a) and Fig.4.2(b), respectively, the output current and output voltage via PSIM and practical experiment are depicted. In order to increase the output voltage, which is close to 47 V, the output current is reduced to 4.57 A. It is evident that a significant DC voltage gain (47/12 V) is obtained, supporting the hypothesis.

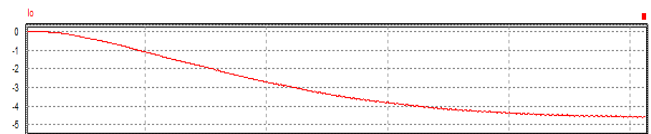


Fig.4.2 (a) Output Current

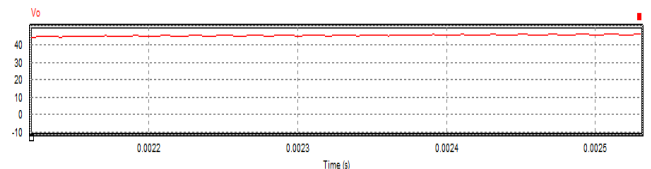


Fig.4.2 (b) Output voltage

C. VOLTAGE STRESS ON SWITCH

Comparing this design to switched inductor and switched capacitor boost converters as well as traditional boost converters, the key benefit is that it reduces the voltage stress on each component. As demonstrated in Fig.4.3 by PSIM, a switch is subject to a voltage stress of 29 volts.

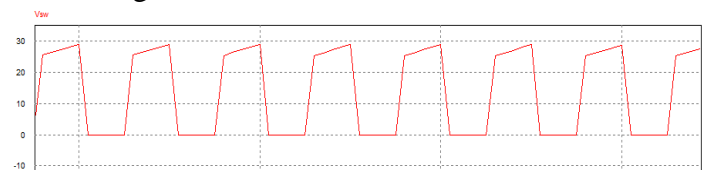


Fig. 4.3. Voltage Stress on Switch

D. PWM SIGNAL WITH DUTY CYCLE

The duty cycle value may be modified to alter the output voltage. The waveform of the PWM signal at various levels, together with the switch signal, are shown in Fig.4.4. A greater duty cycle will result in a broader pulse, which will increase the output voltage.



Fig. 4.4. PWM Signal

E. VOLTAGE STRESS ACROSS DIODES

Voltages across various diodes are shown in Fig. 4.5. VD1 and VD2 represent the same voltage stresses across D1 and D2, respectively, while VD3 represents the voltage stress across D3, VD4 and VD5 represent the same voltage stresses across D4 and D5, respectively.

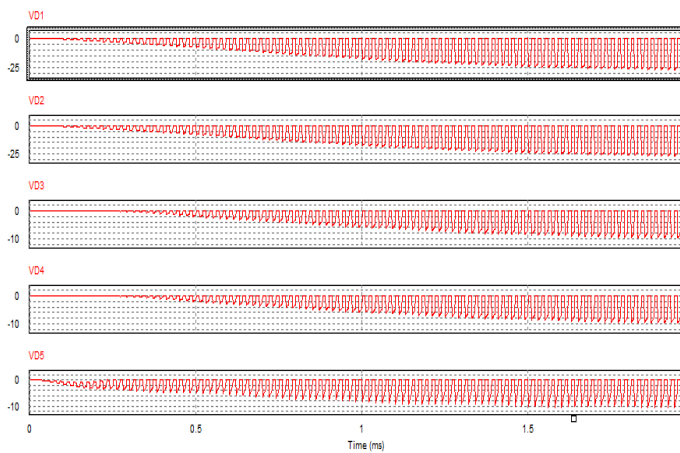


Fig. 4.5. Voltage Stress across Each Diode

F. VOLTAGE ACROSS EACH CAPACITOR

The curve of voltages across various capacitors is shown in Fig.4.6. While VCo is the voltage across the output capacitor that is utilised for filtering, VC1 and VC2 are the same values across C1 and C2, respectively.

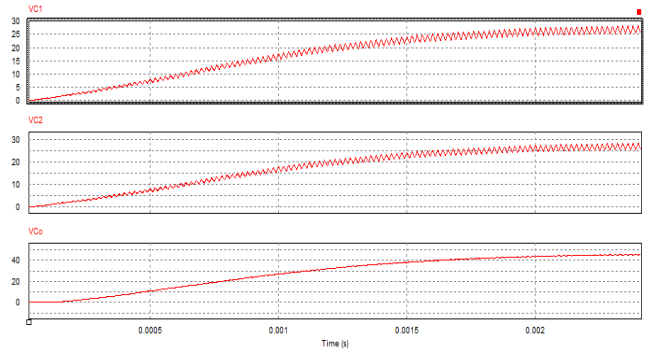


Fig. 4.6. Voltages across Each Capacitor

G. VOLTAGE ACROSS EACH INDUCTOR

The curve of voltages across various inductors is shown in Fig.4.7. While VL2 and VL3 are the voltages across L2 and L3, respectively, and both have the same value due to their parallel connection, VL1 is the voltage across the input L1 inductor.

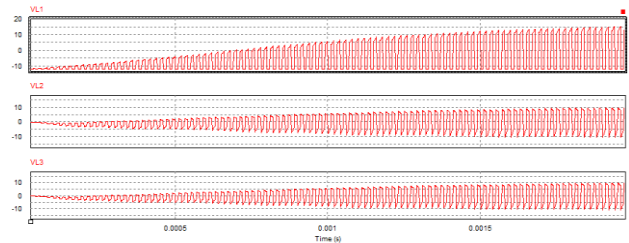


Fig. 4.7 Voltages across Each Inductor

H. CURRENT THROUGH EACH INDUCTOR

The current flowing through various inductors is shown in Fig.4.8. Io is the output current via inductor Lo, whereas IL1 and IL2 are both the same current in values through L1 and L2, respectively.

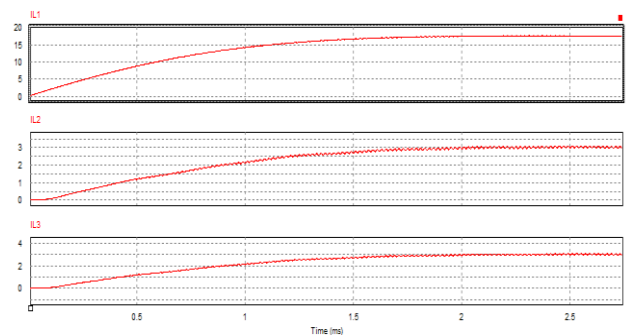


Fig. 4.8. Current through Each Inductor

VI. EFFICIENCY OF THE PROPOSED SLSC DC-DC CONVERTER

After $D=0.55$, the efficiency of the suggested topology leads towards lowering by increasing the duty cycle. The efficiency of the proposed topology improves by increasing the duty cycle when $D>0.1$. Therefore, as shown in Fig. 4.9, we defined the duty

cycle D at 0.55 for the constant frequency of 50 KHz.

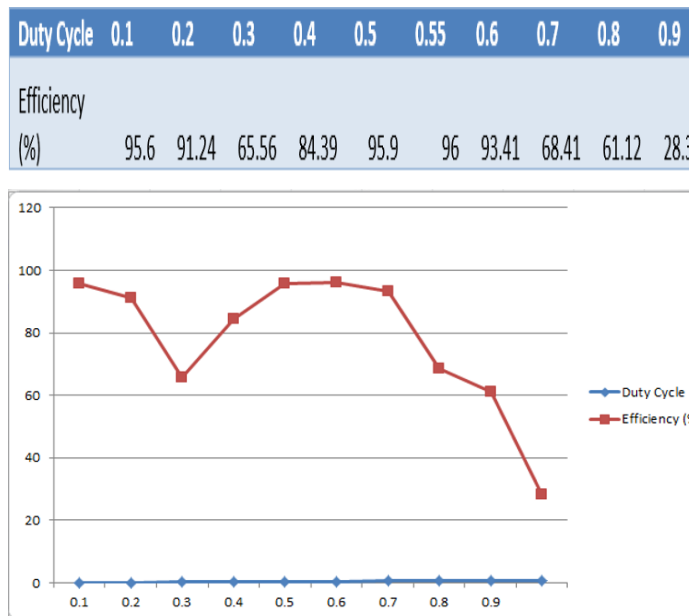


Fig. 4.9. Efficiency of the Proposed Topology

VII. CONCLUSION

This article introduces a ground-breaking High Voltage Gain Hybrid Boost Converter DC-DC converter that significantly outperforms a standard boost converter regarding voltage gain while overcoming complexity and high-duty cycle issues. This converter is a great option for applications like increasing the output voltage of solar panels because of its benefits, like maintaining low-stress voltage, high efficiency, and a wide voltage gain range by turn ratio. The ability to achieve high voltage gain with low-duty cycles ($D = 0.55$), eliminate output diode reverse recovery concerns, and significantly increase voltage gain without changing the inductor turn ratio are some of the key advantages. Successful testing successfully converted a 12V input to a 47V output with 194W of power, matching the results of the computations. DCM analysis, high-power, high-frequency applications, MPPT, droop management in microgrids, and the proposed Z-source converter in inverter mode could all be the subject of future research.

REFERENCES

- [1] D. Lauria, and M. Coppola. "Design and control of an advanced PV inverter." *Solar Energy* 110 (2014): 533-542.
- [2] Basha, C.H. and Rani, C., 2021. Application of Fuzzy Controller for Two-Leg Inverter Solar PV Grid Connected Systems with High Voltage Gain Boost

- Converter. *Journal of Engineering Science & Technology Review*, 14(2).
- [3] Y. Zhang, L. Zhou, M. Sumner, S. Member, and P. Wang, "SingleSwitch , Wide Voltage-Gain Range , Boost," vol. 67, no. 1, pp. 134–145, 2018.
- [4] M. Kumar, M. Ashirvad, and Y. N. Babu, "An integrated BoostSepic—uk DC-DC converter with high voltage ratio and reduced input current ripple," *Energy Procedia*, vol. 117, pp. 984–990, 2017.
- [5] H. Liu, F. Li, and J. Ai, "A Novel High Step-Up Dual Switches Converter with Coupled Inductor and Voltage Multiplier Cell for a Renewable Energy System," *IEEE Trans. Power Electron.*, vol. 31, no. 7, pp. 4974–4983, 2016.
- [6] K. C. Tseng and T. J. Liang, "Novel high-efficiency step-up converter," *Proc. Inst. Elect. Eng.—Elect. Power Appl.*, vol. 151, no. 2, pp. 182–190, Mar. 2004.
- [7] J. Wai, C. Y. Lin, R. Y. Duan, and Y. R. Chang, "High efficiency DC DC converter with high voltage gain and reduced switch stress," *IEEE Trans. Ind. Electron.*, vol. 54, no. 1, pp. 354–364, Feb. 2007.
- [8] R. Nicole, "Title of paper with only first word capitalized," *J. Name Stand. Abbrev.*, in press.
- [9] Y. Yorozu, M. Hirano, K. Oka, and Y. Tagawa, "Electron spectroscopy studies on magneto-optical media and plastic substrate interface," *IEEE Transl. J. Magn. Japan*, vol. 2, pp. 740–741, August 1987 [Digests 9th Annual Conf. Magnetism Japan, p. 301, 1982].
- [10] Veerabhadra, & Nagaraja Rao, S. (2022). Assessment of high-gain quadratic boost converter with hybrid-based maximum power point tracking technique for solar photovoltaic systems. *Clean Energy*, 6(4), 632-645.
- [11] Belhimer, S., Haddadi, M., & Mellit, A. (2018). A novel hybrid boost converter with extended duty cycles range for tracking the maximum power point in photovoltaic system applications. *International journal of hydrogen energy*, 43(14), 6887-6898.
- [12] Hadi, Z. H., Aljanabi, M., Hamza, B. J., & Taha, A. Y. (2023, September). A new MPPT algorithm for photovoltaic system based on hybrid Dingo optimizer and IC algorithm. In *AIP Conference Proceedings* (Vol. 2804, No. 1). AIP Publishing.
- [13] Kulasekaran, P. S., & Dasarathan, S. (2023). Design and Analysis of Interleaved High-Gain Bi-Directional DC–DC Converter for Microgrid Application Integrated with Photovoltaic Systems. *Energies*, 16(13), 5135.